CAST

Status Report to the SPSC for the 127th Meeting and planning for 2018

CERN, October 4, 2017

On behalf of the CAST Collaboration,

editor: Horst Fischer

Albert-Ludwigs-Universität Freiburg
Physikalisches Institut
Hermann-Herder-Str. 3
79104 Freiburg im Brsg.

CERN-SPSC-2017-041 / SPSC-SR-223
13/10/2017

Table of Contents

1 Final Publication on Solar Axion Search

An important milestone reached during this year was the publication of the results of the 2013-2015 data-taking campaign, which can be considered for now as the final outcome of the CAST solar axion programme of the data taken until today. The paper remarked the increase in the sensitivity of the experiment with respect to previous campaigns, thanks to the installation of improved, low-background, Micromegas detectors and a new X-ray telescope, which has allowed CAST to probe, for the first time, the axion-photon coupling down to the most restrictive astrophysical bounds, given by the energy loss of horizontal branch (HB) stars.

The significant improvement in the sensitivity to solar axions in the low-mass part below ~0.02 eV for the last run with evacuated magnet bores over the previous CAST results is presented in Figure 1. The use of Micromegas readouts built with the microbulk technique, out of copper and kapton, and patterned with 500 µm pixels interconnected in *x* and *y*-directions, made possible a reduction of background that led to the best levels ($\sim 10^{-6}$ $keV^{-1}cm^{-2}s^{-1}$) ever obtained in CAST.

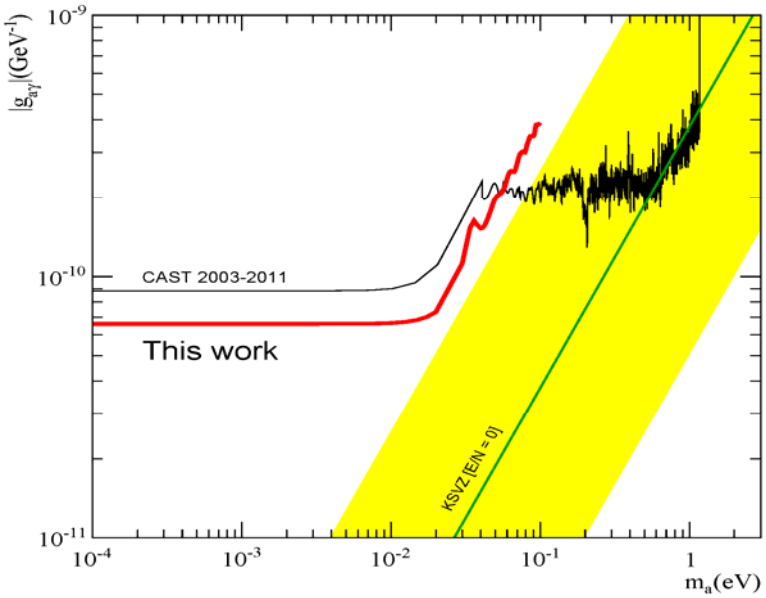

Figure 1: Comparison between the 2003-2011 and the 2013-2015 (labelled `this work') CAST exclusion regions in the m_a - $g_{a\gamma}$-plane.

A clear highlight of the 2013-2015 campaign was the installation in the sunrise system of the first X-ray telescope (XRT) designed and built specifically for axion physics and operated together with a Micromegas detector at its focal point.

The point spread function (PSF) and effective area, i.e. throughput, of the XRT were calibrated at the PANTER X-ray test facility at MPE in Munich in July 2016. These calibration data were incorporated into Monte Carlo geometric ray-trace simulations to determine the expected 2D distribution of solar axion-induced photons, that is shown in Figure 2. Although there is a slight energy dependence on the PSF - the XRT focuses better at higher x-ray energy - more than 50 % of the flux is always concentrated in a few mm^2 area, effectively reducing the background to levels down to ~0.003 counts/h. In addition, the combined XRT and detector system was regularly calibrated in CAST using an X-ray source placed ~12 m away from the optics at the sunset side of the magnet. One such calibration is shown in Figure 2 together with the expected 2D distribution from the ray-trace simulation.

These contours are different from the ones expected from axion-induced photons due to different angular size and distance of the source. The matching between data and simulations confirmed our good understanding of the optics performance.

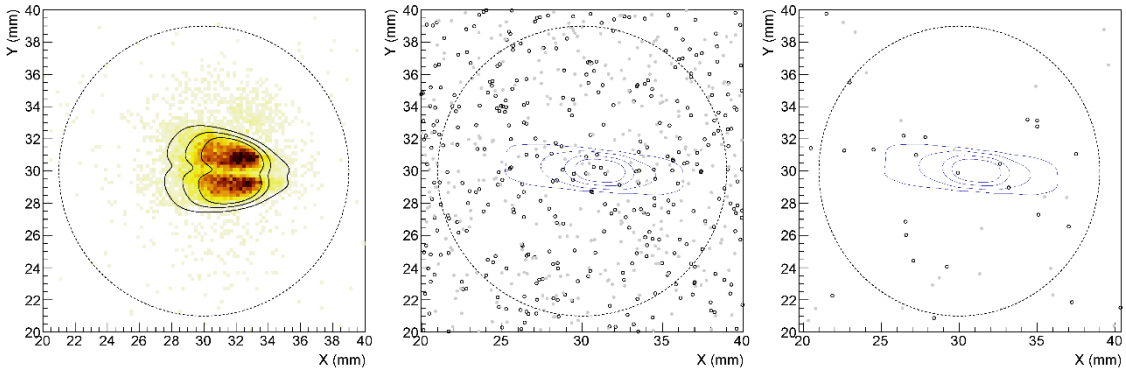

Figure 2: 2D hit map – events detected in the sunrise detector in a typical in situ calibration run (left), as well as in the background (middle) and tracking (right) data. The contours in the calibration run represent the 95%, 85% and 68% signal-encircling regions from ray-trace simulations, taking into account the source size and distance. In the tracking and background plots, grey full circles represent events that pass all detector cuts but that are in coincidence with the muon vetoes, and therefore rejected. Open circles represent final counts. Closed contours indicate the 99%, 95%, 85% and 68% signal-encircling regions out of detailed ray-trace simulations of the XRT plus spatial resolution of the detector. The large circle represents the region of detector exposed to daily energy calibration.

The results published in *Nature Physics* corresponded to 1132.6 (hour detector) of data taken in axion-sensitive conditions, i.e. magnet powered and pointing to the Sun, in 2013, 2014 and 2015. In 2013, only sunset detectors were operative, while in 2014 and 2015 both the sunset detectors and the new sunrise system, installed in CAST in September 2014, took data. The final result was an upper limit in the $m_a < 0.02$ eV range for the axion-photon coupling $g_{a\gamma} < 0.66 \times 10^{-10}$ GeV^{-1} at 95 % C.L.

This constraint considers only statistical fluctuations in the tracking data, while overall systematic effects were estimated to be well below 10 % of the quoted result. The paper was sent to the journal in January, accepted in March, and published online, as an open-access paper, on 01 May 2017 as https://www.nature.com/nphys/journal/v13/n6/full/nphys4109.html (doi:10.1038/nphys4109).
A review by Maurizio Giannotti appeared in the "News and views" section of the same volume several blogs and journals such as,
https://phys.org/news/2017-05-important-milestone-axion.html,
http://spaceref.com/astronomy/cast-project-places-new-limitations-on-dark-matter.html,
http://cerncourier.com/cws/article/cern/68774 (June 2017 edition)
and many other web pages at different Universities and institutions picked up the news.

2 Status of CAST Infrastructure

2.1 Integration Studies for RADES and CAPP cavities

A series of calculations for the forces and the temperature increase induced to the two cavity types during a quench have been launched by EN-MME, taking into account the magnetic field transient from data of an actual quench (9/10/2015).

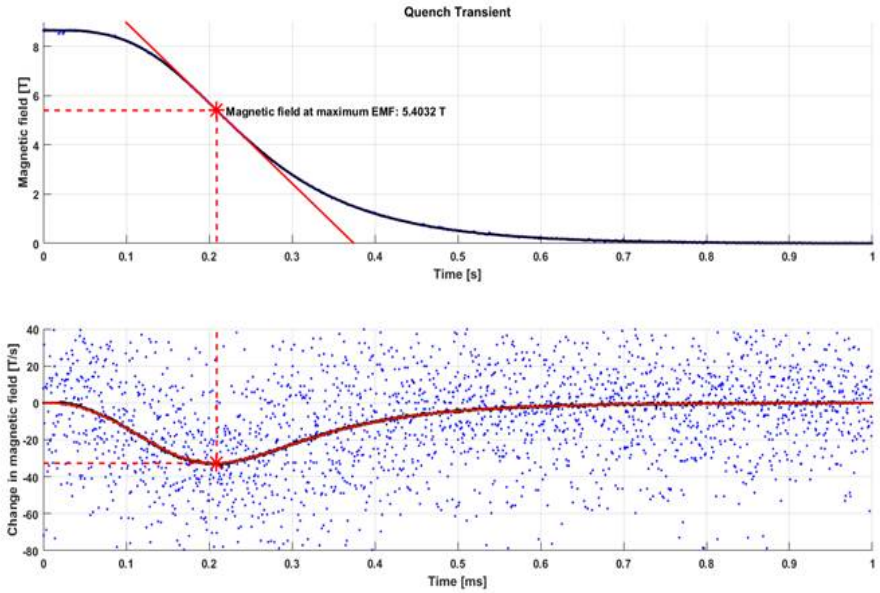

Figure 3: Timeline and transient of the magnetic field during the quench of October 9, 2015.

For the calculations the following assumptions have been made:

- Homogeneous magnetic field passing orthogonally through the base area of both cavities.
- Perfect electrical contact conductance between cavity halves (this is a conservative assumption) for the CAPP cavity.
- Both inside and outside coated in Cu (30 microns; conservative value).
- The cavity geometry was simplified as three separate “coils”:
    - The outer copper layer,
    - the bulk steel wall,
    - the inner copper layer.

2.1.1 Results - RADES

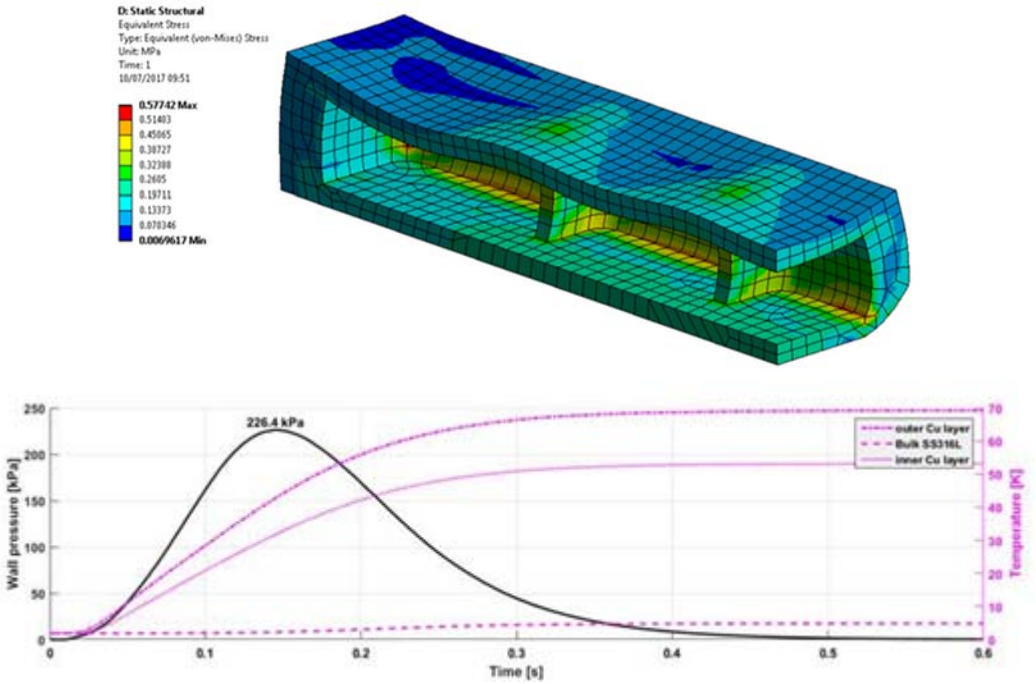

Figure 4: (Top) The sum of the contributions of the 3 "coils" results in wall pressure of up to 88 kPa which acts orthogonal to the cavity wall (outwards). The resulting stress of 0.578MPa is very low. (Bottom) The most significant temperature increase is recorded in the outer copper layer, with a final ~70K. This corresponds to a thermal strain of about 0.018% (assuming that steel remains at the initial 1.9K). With reasonable adhesion of the copper layer this appears to be acceptable. The cooling of the cavity due to the 1.9K environment is not taken into account.

2.1.2 Results - CAPP

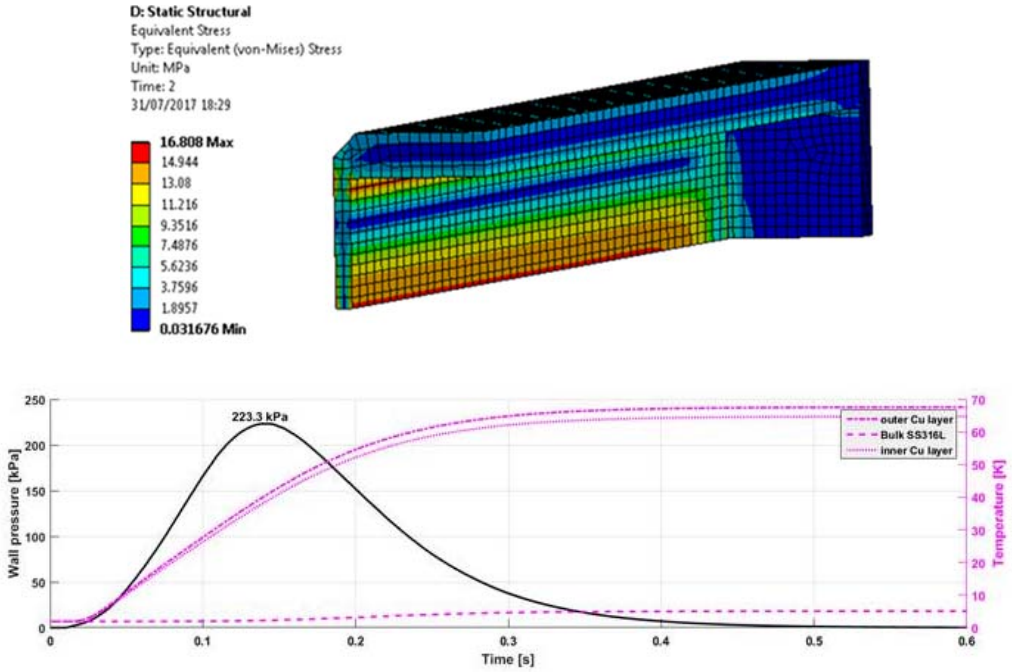

Figure 5: (Top) The limit for 316L is at least 225 MPa (after which some local plastic deformation may occur). In this cavity, at 223.3 kPa wall pressure (which is the worst case with perfect electrical conduction and 30micron layers on both sides of the steel wall), the resulting stress is 16.8 MPa. (Bottom) The total current is higher than in RADES, but distributed over a larger cross-section, that is why the temperature increase as well as the resulting pressure due to Lorentz forces is about the same.

2.1.3 Conclusions

The studies have verified that the implications of the quench on the cavities are well within the tolerances of the particular cavities. The results have been discussed with experts from TE-MPE and the induced current to the 3 “coils” of the cavities will not pose any threat to the magnet. Nevertheless, as an extra precaution we were advised to ramp up in stages and quench the magnet in mid-field values, as a conservative approach.

3 Magnet Intervention

A maintenance of the vacuum system was required in 2017, namely several gauges needed to be replaced and the primary pump of the InGrid detector vacuum line was sent for revision.The intervention on the MFB side to thermally isolate the cold bore pipe from the gate valve pipe at the level of the 3He cryogenic window flange has been successfully completed. The MFB bellow was closed on the 22nd of May.

On the MRB side the 2K return pipe has been redirected in order to have enough clearance for the vacuum vessels which will house the amplifiers and the signal feedthroughs (Figure 6). After revising the instrumentation, the MRB end flange of the magnet was closed with the help of the TE-CRG group.

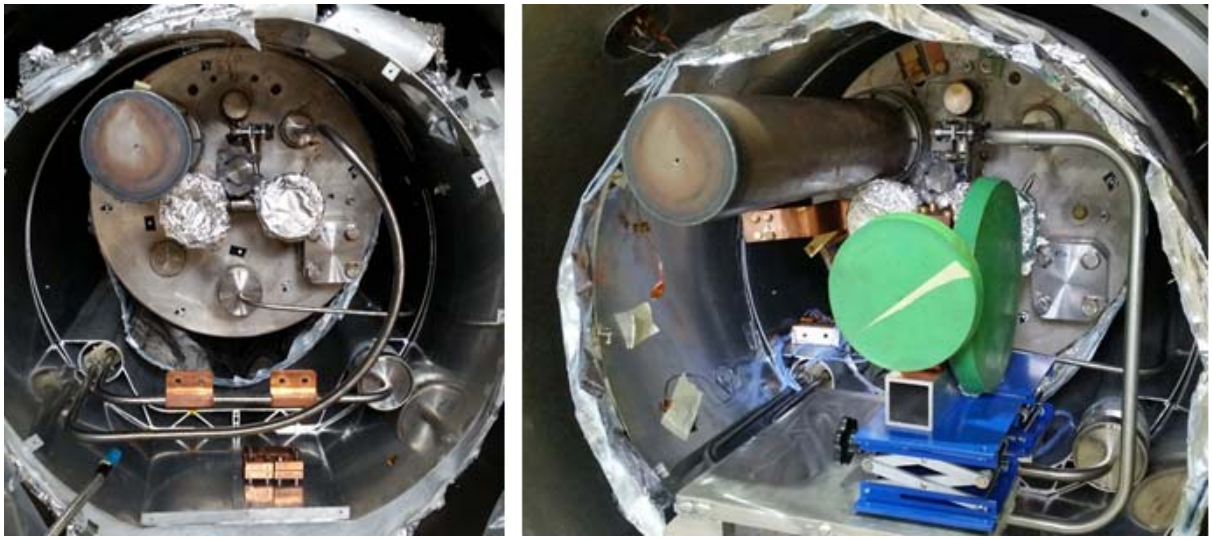

Figure 6: The modification of the return pipe of the CAST magnet was necessary to fit two signal feedthrough vessels for the two types of cavities.

The upgrades of the infrastructure (new counter weight platform for R&D of KWISP detectors on the MRB side, new equipment, cables, etc.) were completed by the 8th of August.

4 Cryogenics and ABB Upgrade

The ABB migration is officially finished, in the future Cryo group will do some electrical/mechanical consolidations but this actions remain as a standard activity that is done normally for maintenance and consolidation.

The cool down has started on the 18th of August. The reason for the delay was the work needed after the accident of the 24th of August with the magnet. The Cryo operators managed to cool down the magnet at 1.8K on the 28th of September and started checking the recovery ability in case of shut

down, re-connection and quenches. We expect the CRYO OK signal latest on the 6th of October and are planning the quench training on Monday the 9th.

5 Schedule and CAST planning

The baseline schedule was interrupted by the accident of August with the magnet and the incident in September on InGrid. We expect to receive the CRYO OK signal, which will allow us to ramp up the current, in the following day and start with the quench training of the magnet in the following days. During the cooling down of the magnet we will be working in parallel on the InGrid vacuum line.

The delay from the original schedule is estimated to 3.5 weeks mainly due to the accident with the CAST Magnet during the KWISP 2.0 data taking in August.

The present run with InGrid/KWISP 2.0 and RADES will start on the 15th of October and continue until the 25th of March 2018. Between the 13th and the 25th of March we will have the Sun filming measurements. On the 26th of March the preparations for the shutdown of CAST will start. The proposed layout for CAST in 2018 is shown in Figure 7 and the preliminary planning (not consolidated) of the interventions is shown in Figure 8.

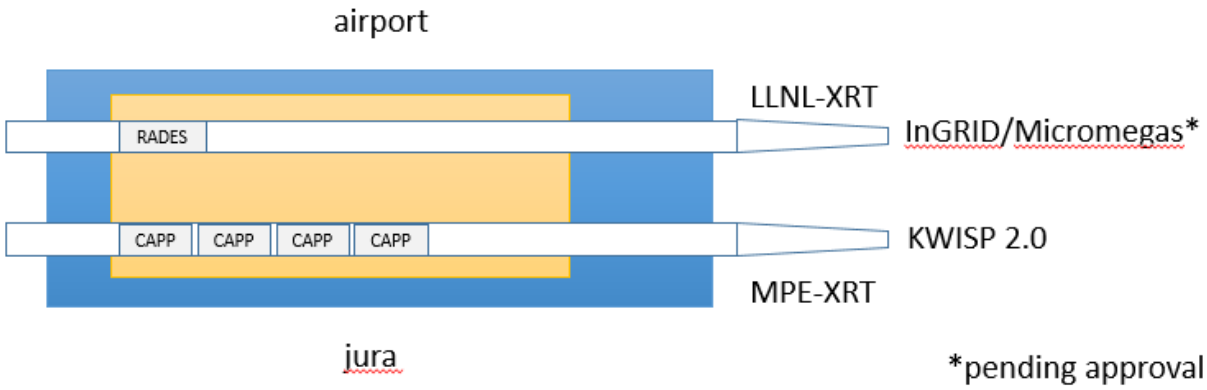

Figure 7: Proposed setup of CAST for 2018.

After removing the RADES cavity we will verify the position of the spot on the InGrid detector with an X-ray finger run. The installation and alignment of the Micromegas detector will follow. Then KWISP 2.0 will be installed behind the MPE X-ray telescope. Two major upgrades are planned for the detector lines in 2018:

- Redesign of the KWISP 2.0 detector line for parallel running with X-ray detectors in the airport line of the sunrise platform.

- Modification of the 3He gas system and control software to circulate Xenon as detector gas for the Micromegas detector run.

We are investigating an upgrade in the temperature monitoring instrumentation of the MFB side together with the Cryolab. This intervention can be performed in parallel with the other activities. It is not compatible only with moving the magnet. The shutdown will also contain the usual cryogenics and vacuum maintenance.

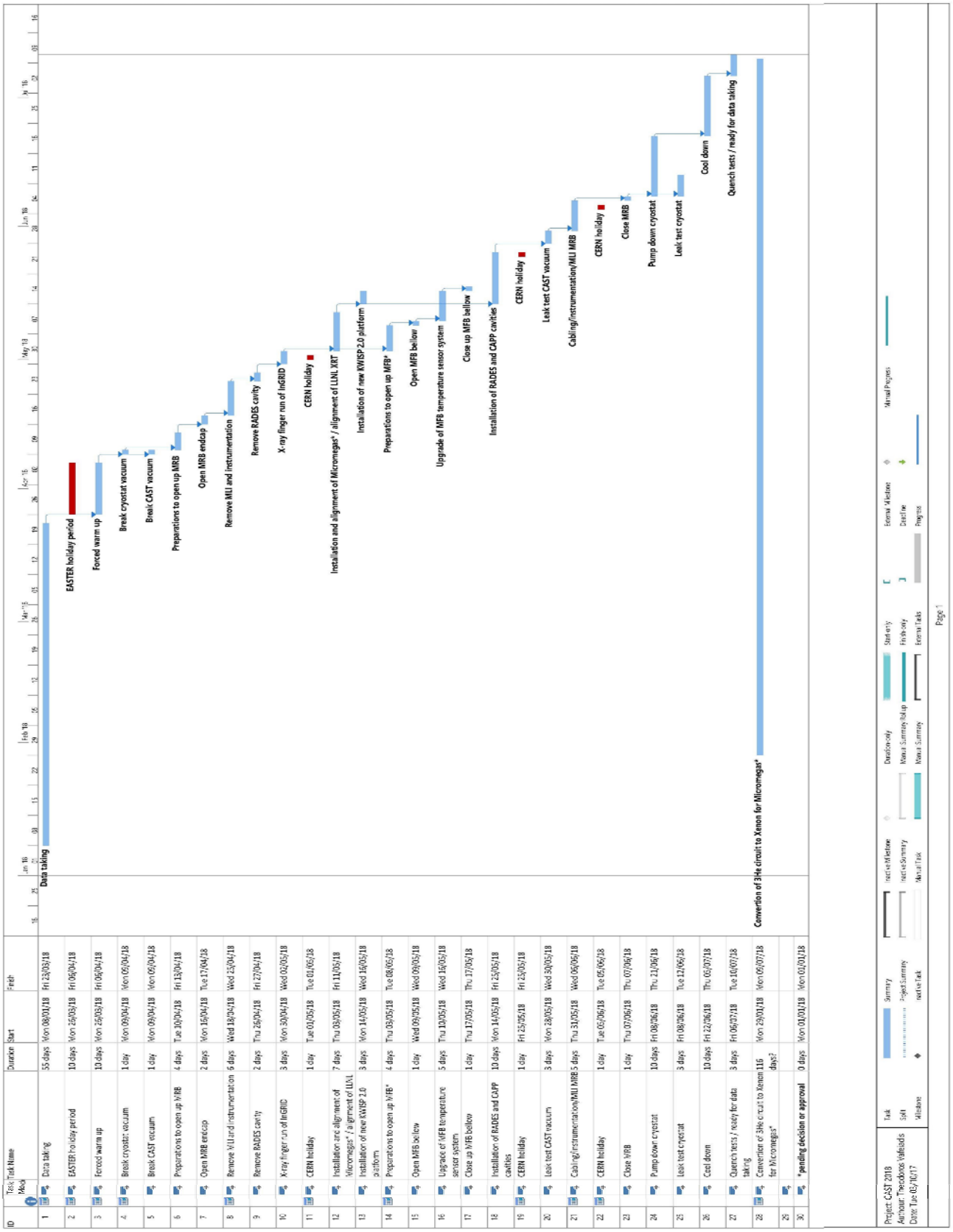

Figure 8: Preliminary planning of 2018.

6 Detectors: InGrid

6.1 The Septemboard Detector System

The upgrade program of the detector has been finished and a new detector had been built. The problems observed last year with sparking InGrids could be solved. A new USB-SPI-based temperature monitoring system has been implemented. A temperature sensor on the backside of the Septemboard indicated temperatures of more than 75°C for a board equipped with only 5 InGrids. A clear dependence of the temperature on the length of the open-shutter time per event could be demonstrated, by varying the time between 100 µs and 1 s and observing a temperature variation of 10°C. Forced airflow cooling of the detector's backside could reduce the temperature by 10°C (see Figure 9). At the same time, the spark rate was reduced by one order of magnitude. Further reduction of temperature by another 10°C through improvised cooling measures made the sparks almost stop completely.

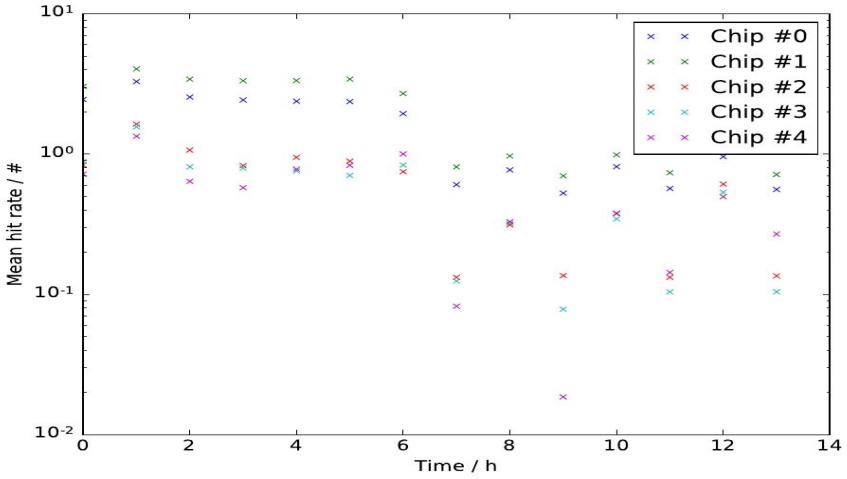

Figure 9: Decrease of hit rate in detector, after switching on forced air flow cooling (at 6.5 h after start).

A water cooled heatsink has been designed for the detector. It is made from copper and features a cooling channel with 3 mm diameter directly below the Septemboard (see Figure 11). For production, two oxygen free copper plates were produced, one with the pipe carvings and one as a cover. Both plates were joined by brazing in a vacuum oven with a 50 µm thin brazing foil in between (final heat sink see Figure 10). The design, proven to be water tight, could keep the chips at a desired temperature of 45°C, even at CAST-required readout frames of 1s. As a cooling agent deionized water is used, which is circulated by a PC cooling setup consisting of a pump and a large radiator. The setup should in principle be able to dissipate more than 50 W which is definitely sufficient for a maximum 10 to 15 W produced by a Septemboard.

Because of the new water cooled heatsink several parts of the detector had to be redesigned and produced. In particular the drift cylinder with the field cage and several inserts separating the grounded heatsink from signal and power lines and especially the HV lines were necessary. The completed detector was assembled in July and was tested in Bonn for functionality (see Figure 12)

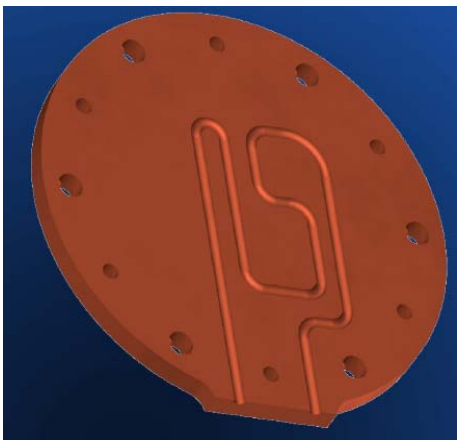

Figure 10: CAD model of the cooling plate with pipe. carving

Figure 11: Cooling plate after reflow soldering.

Also problems with the other components of the upgrade program could be solved:

1.) The large scintillator above the lead shielding: This detector designed to record cosmics passing through the detector or the beamline during an event was tested during the data run in December 2016. It was however observed, that the setup produced a high rate oscillation with high amplitude, which rendered the device useless. In the lab, this effect could be reproduced and it was found out, that a faulty grounding scheme was causing this. After improving the grounding, the setup could be operated without problems in the lab.

2.) Piggy-back scintillator on the detector behind the GridPixes: The existing circuit could be verified and it was included in the upgrade of the readout PCB closing the detector (intermediate board) together with the above mentioned temperature readout. A reliable operation has been demonstrated while operating the scintillator independently of the InGrid readout. It was also tested, that the scintillator circuit has no impact on the GridPix readout. However, when combining the two readout streams in the FPGA, several unexpected signal shifts and delays were observed. This could be solved shortly before the installation, but final tests of a combined readout are still pending.

3.) Thin SiN windows: A design featuring 300 nm thick SiN membranes in combination with a strongback consisting of four 500 µm wide Si ribs showed good reliability and pressure stability. Each of the three windows of the first production cycle withstood several pressure cycles with 1.5 times the nominal pressure differences (1050 m bar) and one was tested 18 times with pressure differences of at least 1 bar. The Helium-leak rate was determined to be smaller than 8×10^{-8} mbar l/s for all three windows. One of these windows was also used in the data taking period in December. However, a second batch did not show such a good performance and several windows burst at significantly lower pressure differences. Since diverging results are reached from tests at NORCADA and in Bonn, a new bracket design was made, to allow tests at both locations with the identical windows. First samples are being produced and tested at NORCADA currently and will be sent to Bonn soon for testing.

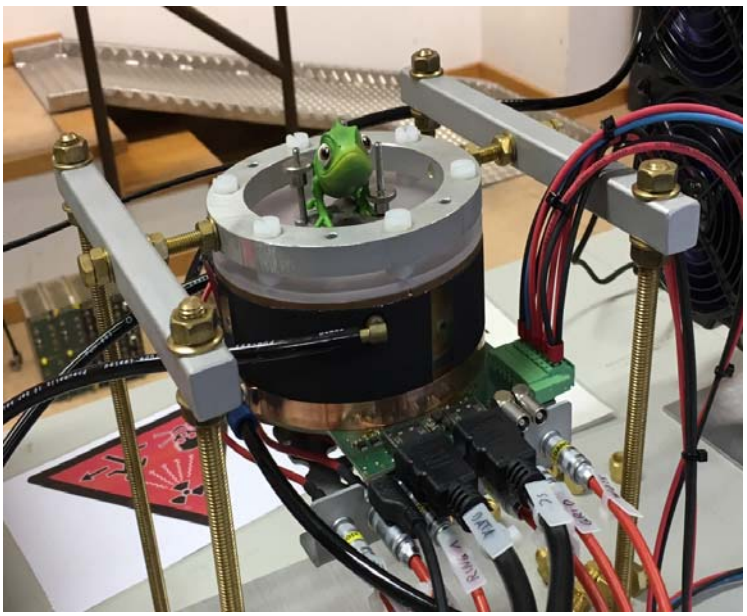

Figure 12: CAST detector during final tests in lab at Bonn.

6.2 Installation of LLNL telescope

The LLNL X-ray telescope was installed and aligned with a theodolite in the V2 bore of the sunrise side, to focus the converted X-rays towards the InGrid detector. We installed in total 17 fiducial stations on the telescope, along the beam pipe and on the detector. The surveying team (EN/ACE) measured their position with respect to the coordinate system of CAST. Alignment with the theodolite will not be possible once the RADES cavity is installed therefore the fiducial positions will be used to verify the alignment of the detector system

6.3 Installation in CAST

As planned the detector was mounted on the X-ray telescope in mid-July so that the alignment could be checked with the laser beam from the Jura side of the experiment. The geometers measured the position of the detector and both an X-ray finger run as well as two days of data taking with full lead shielding could be done. The shielding was slightly modified to fit the detector and the cables. Then the detector was unmounted to clear the space for KWISP data taking.

The remounting of the detector started on 10.9.2017. During the commissioning it was observed, that the cooling did not work. During the investigation it was found out, that rubber fragments had blocked the water inlet at the heatsink, which is a 90° connector screwed into the cooling channel and presents a bottleneck.

The rubber fragments stemmed from rubber gaskets inside the self-locking quick couplings used to connect the heatsink to its cooling device. These quick couplings have therefore been replaced by standard Swagelock connectors. By injecting pressurized air the cooling path could be cleared and a sufficient flow has been reestablished.

During such an operation, accidentally, pressurized air was introduced into the detector which led to a burst of the 300 nm SiN-window into the vacuum line. A thorough investigation of the consequences

of this incident has been made and we found some indications that the Septemboard suffered from mechanical stress. As a matter of precaution the board has been exchanged against a spare board.

The pressure at the linear gauge connected to this line went up to ~200 mbar. The debris of the window (dust of a few nm) are believed not to have damaged the telescope. Some scratches may have occurred but this will not influence the overall efficiency of the telescope.

To exclude possible contamination of the vacuum line and X-ray telescope, caused by the compressed air, the TE-VSC have been requested to take a swipe sample from the inner part of the vacuum line. From the report, the level of purity of the analysed elements is close to the criteria of acceptance for UHV applications at CERN. The weak traces of existence of hydrocarbons are coming from the manipulation of the vacuum pieces, from cleaning them with acetone or ethanol contained in plastic bottles or from the ambient atmosphere. In comparison the contamination from several litres of compressed air in the system is negligible.

A ^{55}Fe source which is used for the calibration of the detector was inside the vacuum line and may have been hit by the pieces of the window. The RP has inspected the source and confirmed it was not damaged. A sample has been collected for further analysis. The results were negative.

6.4 Course of actions

The pipes of the cooling system and the gas system of the detector although labelled they had the same colour and the same fitting. The necessary changes will be implemented. An interlock exists that closes an electro valve at the inlet of the gas of the detector in the event of pressure increase at the telescope. We will add two electro valves that act on the same interlock and they will isolate the detector chamber. Before the installation of the pipework and detector system, the leak tightness of the gate valve to the magnet cold bore was tested for leak tightness and the region of the telescope flushed with Nitrogen several times. No leak was found. We are confident that the system will be operational by the 15th of October at the latest.

6.5 The analysis of the 2014/2015 data

A paper on the detector performance during the data taking run has been published under the title *A GridPix-based X-ray detector for the CAST experiment* in Nucl. Instrum. Meth. A **867** (2017) 101 (doi:10.1016/j.nima.2017.04.007). A second paper (*Energy Dependent Features of X-ray Signals in a GridPix Detector*, arXiv:1709.07631) on the data taking in the CAST Detector Lab has been submitted for publication to Nucl. Instrum. Meth. A.

The search for solar chameleons using the InGrid data of 2014 and 2015 got closer to finalization. The few details missing, like XRT parameters, could finally be fixed. The list of sources for systematic uncertainties has been completed and fixed recently. What is now only left is the proper estimation of the different contributions to the systematic uncertainties which up to now have only been estimated very conservatively. For each contribution a clear strategy for the proper estimation has been identified/defined. Figure 13 shows the final observed spectrum in the energy range of 0.2 keV to 2 keV in the innermost chip region. The data points are compatible with the background confirming the expected upper limit on β_γ of $5.6 \cdot 10^{10}$, displayed in Figure 14 with the previous CAST limit as comparison, thus the potential to surpass the solar limit of $\beta_\gamma = 6.457 \cdot 10^{10}$. The calculation of the observed limit will be performed once all systematic uncertainties are fixed. Work on the publication has started lately.

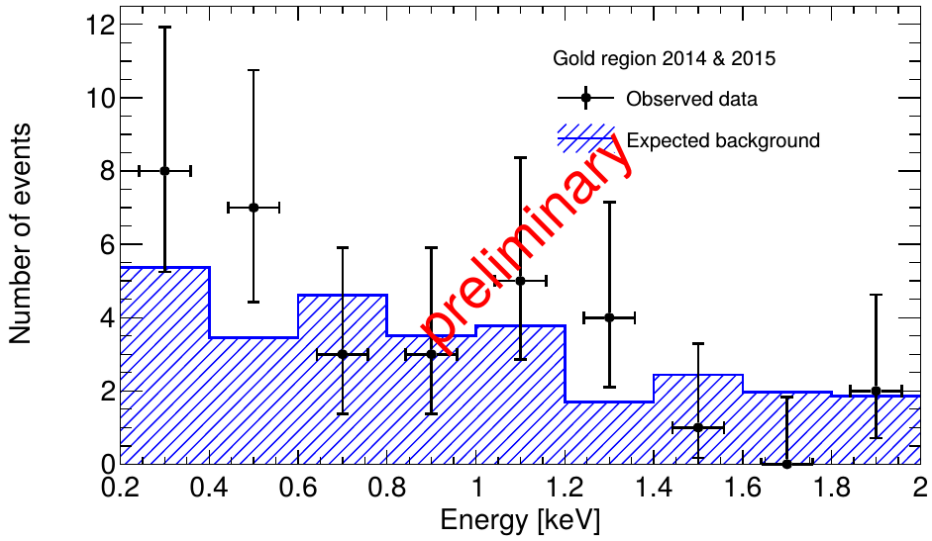

Figure 13: Final spectrum in the energy range 0.2 keV to 2 keV.

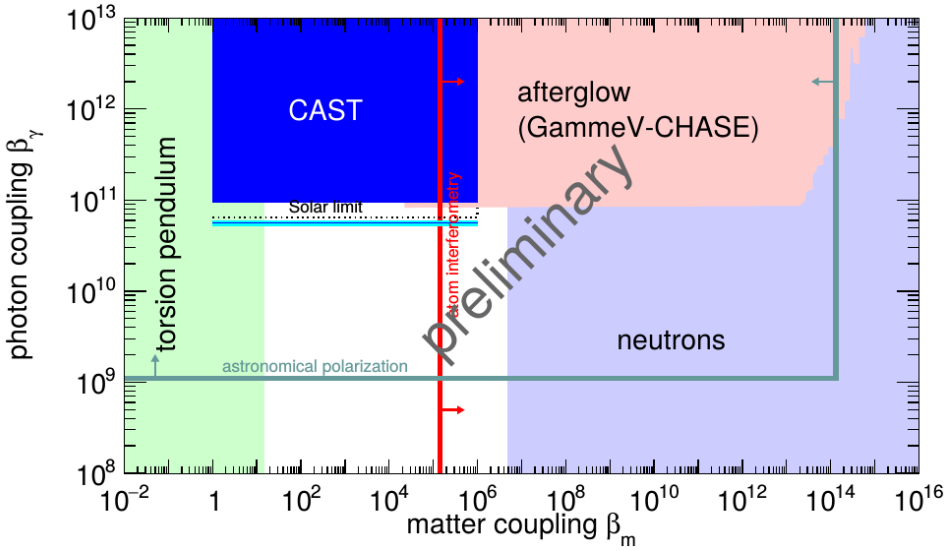

Figure 14: Expected upper limit of this analysis in comparison to other limits.

7 Detectors: KWISP

7.1 Status of the KWISP 1.5 detector

The so called KWISP 1.5 detector has performed a first measurement in December 2016. The occasion was related to the alignment of Sun with the galactic center when an enhanced flux of chameleons due to the gravitational lensing could be expected. The first on-beam live data taking has pointed out deficiencies in the experimental setup that were addressed later and upgrades have been made for the following data taking runs.

The KWISP 1.5 detector is basically a Michelson type interferometer with a homodyne readout (see below).

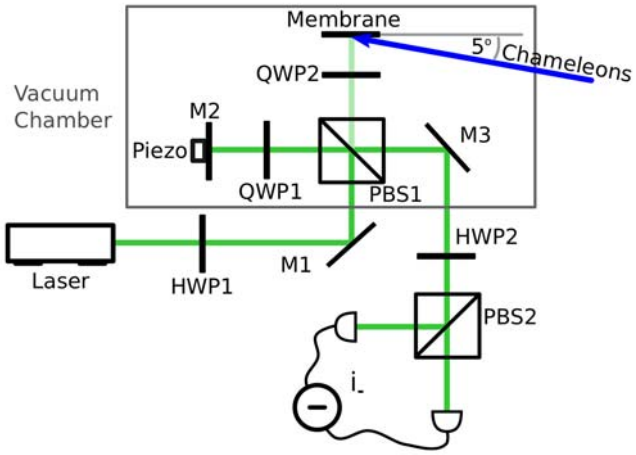

Figure 15: Scheme of the experimental setup with homodyne readout of the interferometer.

The membrane which is sensitive to the chameleon stream is acting as one of the mirrors in the Michelson interferometer. The light reflected from the membrane is combined in the polarizing beam splitter (PBS1) with the light coming from the reference arm. The PBS1 in combination with two quarter wave plates (QWPx) functions as an "one way valve for the light" and prevents the light from the interferometer to propagate back to the laser. In this way all the light from the interferometer which carries the information on the position of the membrane is directed towards the balanced homodyne detector. The beam that consists of two orthogonal polarizations is combined and divided in two equal parts with the half wave plate (HWP) and PBS2. The two beams after PBS2 are transformed into electrical signal by two equal photodiodes. The currents coming from the photodiodes are subtracted, transformed into voltage signal and amplified. In appropriate conditions, when the phase difference of the beams in two interferometer arms is 90 degrees, the voltage contains the information on the membrane condition. The advantage of such a readout scheme is that it rejects correlated noise in two beams. Furthermore, the beams propagate on different paths only inside the vacuum chamber thus greatly reducing the noise.

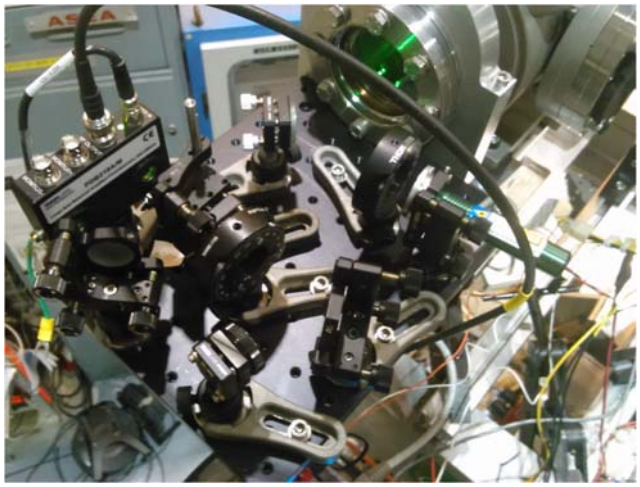

Figure 16: Optical breadboard of the KWISP 1.5 setup. Laser on the right and balanced homodyne detector on the left can be seen.

Also, the chameleon chopper was mounted between the telescope and the sensor in order to create a time dependent chameleon flux.

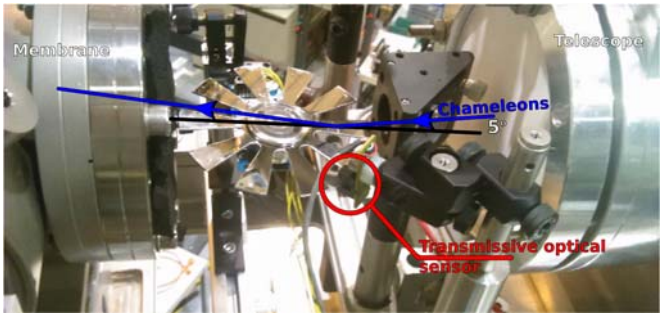

Figure 17: Cut out chopper wheel capable of reaching rotation frequencies up to 55 Hz. This traduces to 550 Hz in the chameleon signal.

The angle with respect to the beam was chosen to be the same as the sensor's angle since the membrane and the chopper wheel material have similar densities and thus reflecting chameleons in the same energy range. The accessible region is shaded one, where the maximum coupling constant represented by a solid horizontal line is somewhat arbitrarily taken.

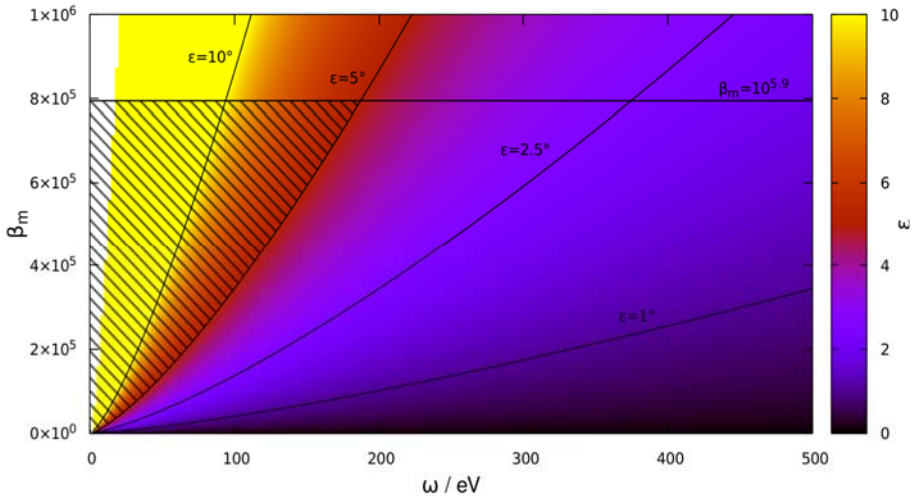

Figure 18: Accessible region in the chameleon coupling constant to matter versus chameleon energy. The experiment is sensitive to chameleons in the shaded region to the left of the five degree line.

After upgrades and debugging a second engineering run has been done in February 2017. The control of the system including a feedback loop and data acquisition is done on a silicon on chip single board computer which can be controlled over network interface. A graphical user interface was written and the system has become fully integrated and user friendly. A great care was taken to assure no data is lost during various steps in the transfer since every lost byte enhances the noise level in the signal as simulations have confirmed. The software development was frozen and work on the mechanics upgrade has started since an acoustic pickup on the membrane was detected and a series of interventions were made on shielding and mechanical decoupling of the sensor from the environment including the chopper. During April 2017 a new engineering run took place and also the mechanical design was frozen. This lead to a data taking campaign in June during which minor adjustments on the setup were made. The run produced data with the **so far best sensitivity (10^{-12} m/√Hz)** and the preliminary plots can be seen below. The signal is expected at a frequency of 984.4 Hz and in the lower plot no signal is visible during 10 hours of background measurement at approximately 10^{-11} N.

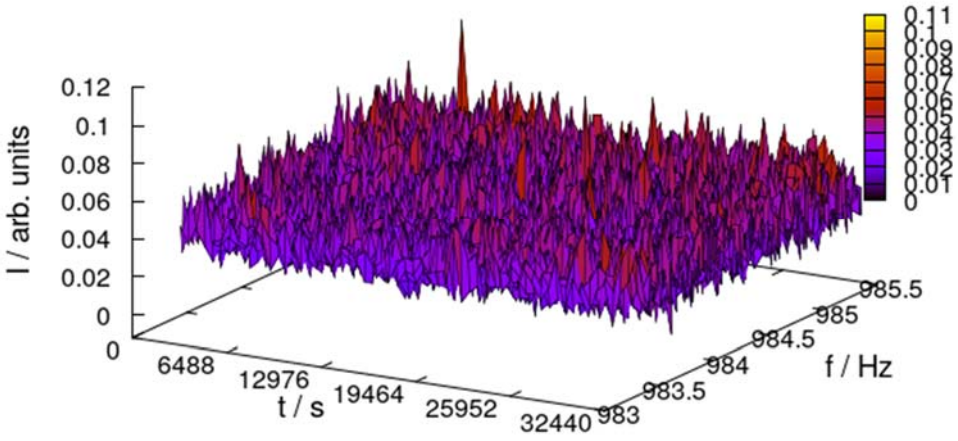

Figure 19: Time resolved spectrogram. Plot refers to background data taken on the 02.07.2017. The data stream is ten hours long.

The picture remains the same during tracking. Also in this case, no signal is observed above the background at a chopper frequency.

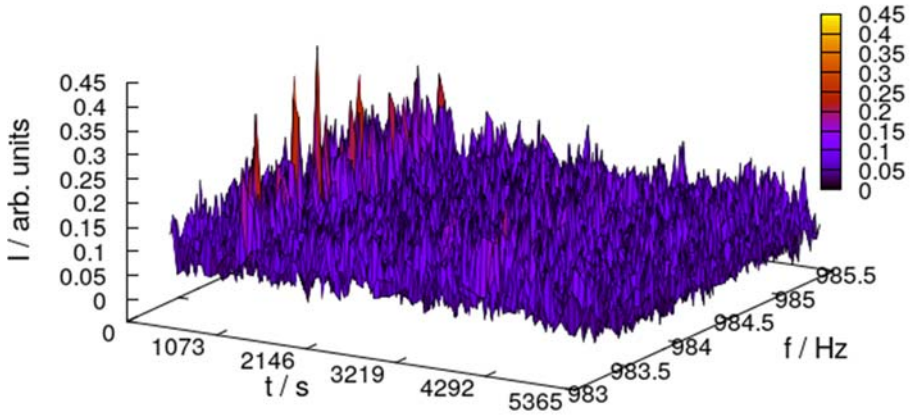

Figure 20: Solar tracking data taken in the morning of 03.07.2017. No peak at the expected frequency is visible. Data stream is ninety minutes long.

In conclusion a fully working and integrated system was built, tested during a month of on beam time and at least a set of scientific data was acquired. Analysis and interpretation of the data is currently in progress.

7.2 Status of the KWISP 2.0 detector

The laser powering the KWISP 2.0 detector was finally returned from the manufacturing company in the second half of July 2017. This unit had been sent back to the company in February 2017 to check the emission line-width, measured by us to be a factor almost 10 larger than specified, and the malfunctioning temperature tuning control. The laser was checked for performance in the CAST preparation lab and we found that the repairs had actually brought the line-width within a factor 2 of the specifications. After checking the laser performance, the Fabry-Perot cavity of the detector, with the sensing membrane inside was placed in the laser beam. To estimate the sensitivity of the detector to membrane displacements, a sine-wave signal was applied to a piezo actuator displacing the membrane cavity longitudinal axis, simulating the action of an external force acting on the membrane. From this calibration, based on the nominal characteristics of the piezo chip used, we estimated a sensitivity of 2.7×10^{-10} m/√Hz.

The KWISP 2.0 detector was subsequently installed on the CAST magnet and aligned with the sensing membrane positioned in the focal plane of the ABRIXAS telescope. The membrane is tilted at a 5˚ grazing angle with respect to the expected incoming solar chameleon beam. The breadboard housing the membrane sensor and its readout optics is mounted on special "sorbothane®" rubber feet to passively isolate it from mechanical vibrations.

The chameleon chopper was positioned to intercept the chameleon beam emerging from the telescope and was fixed to a structure mechanically decoupled from the membrane sensor. In order to minimize acoustic noise the chopper was equipped with a solid wheel having 20 alternating rough and smooth sectors. A triggering tab was also placed on the chopper wheel to measure the chopper actual frequency with an external opto-coupler.

The entire assembly, chopper included, was enclosed within a heavy rubber shielding designed to suppress acoustic disturbances. The shielding consisted of 1 cm thick rubber sheets mounted on an aluminum frame resting on "sorbothane®" rubber feet.

Figure 21: Top view of the KWISP 2.0 sensor installed on the CAST beamline with the shielding removed. The vacuum chamber holding the sensing membrane is visible at the center, with the chopper wheel at its left. The hypothetical chameleon beam impinges from the left after passing through the X-ray telescope

Figure 22: Bottom-up view of the KWISP 2.0 sensor installed on the CAST beam-line with full shielding. The hypothetical chameleon beam impinges from the right. The X-ray telescope external tube is visible at center-right.

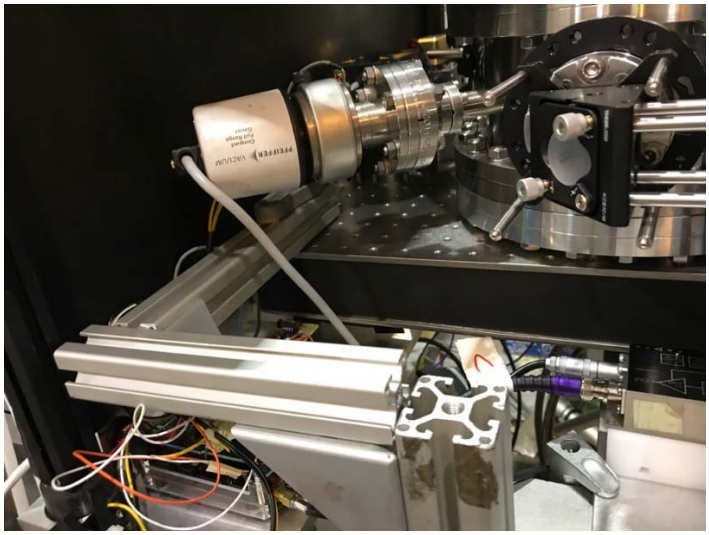

Figure 23: Close-up view of the aluminium profiles supporting the chopper assembly. Note the gap, visible at center, between the profiles and the top of the optical breadboard ensuring mechanical decoupling.

Figure 24: View of the chopper wheel.

Data acquisition was performed using the same system employed for the KWISP 1.5 detector, including the external control and monitoring of the chopper frequency. We acquired the signal from the photodiode monitoring the light transmitted through the Fabry-Perot cavity and the AC part of the error signal generated by the electro-optic feedback loop which keeps the cavity and the laser under lock. The latter signal contains the information on time-varying membrane displacements. Acquired data are stored for off-line analysis. Data analysis consists basically in performing a Fast Fourier Transform (FFT) on the AC error signal to search for membrane displacements at the chopper frequency, where a hypothetical chameleon signature should appear.

The KWISP 2.0 detector in the configuration briefly described above was used for a pilot sun-tracking live data taking run at the end of August 2017.

7.2.1 August 2017 – sun-tracking run statistics – KWISP 2.0 detector

Total tracking data acquisition time = 11700 s
Total background data acquisition time = 10800 s (5400 s chopper ON, 5400 s chopper OFF)

Figure 25 shows a sample spectrum of the AC error signal from a calibration run, when the membrane was displaced in a controlled way using a sine-wave signal. The peak visible at 833 Hz is corresponds to a displacement of 17 nm of the membrane along the cavity longitudinal axis. With this calibration, again based on the nominal characteristics of the piezo chip used to displace the membrane, we estimate from the background level a sensitivity of ~10^{-9} m/√Hz

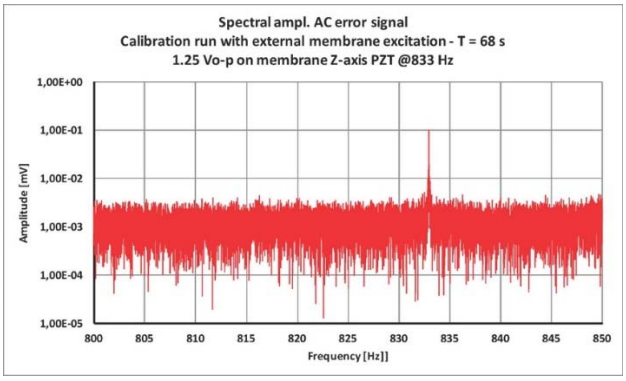

Figure 25: Spectrum of the AC error signal from a calibration run.
Note the peak visible at the membrane excitation frequency of 833 Hz (see also text).

Figure 26 shows sample spectra of the AC error signal from a background run with the chopper ON and OFF respectively. During background runs the magnet was stationary and in its horizontal parking position. The frequency region is chosen around the chosen chopper frequency at 843 Hz.

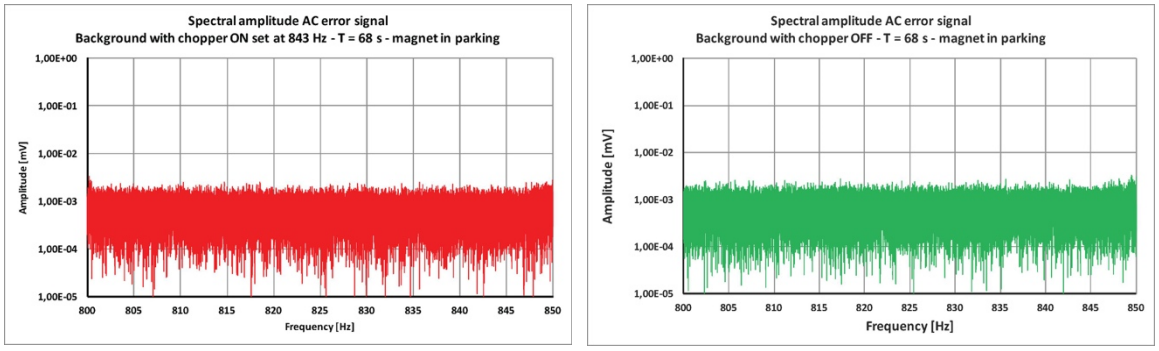

Figure 26: (left) Sample spectrum of the AC error signal from a background run with the chopper ON set at 843 Hz. (right) Sample spectrum of the AC error signal from a background run with the chopper OFF set at 843 Hz. Note that no peak is visible at the chopper frequency (see also text).

Figure 27 shows a sample spectrum around the 843 Hz chosen chopper frequency from a sun-tracking run. Note that no signal is visible at the chopper frequency and that the background level is comparable to that observed during background runs.

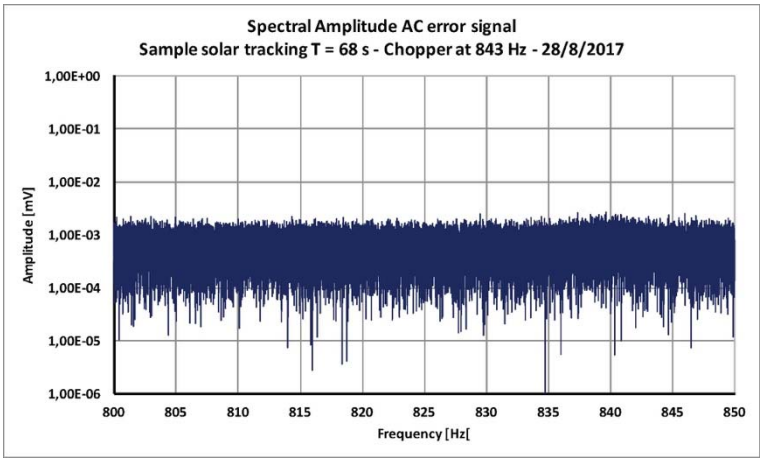

Figure 27: Sample spectrum of the AC error signal from a live sun-tracking run with the chopper set at 843 Hz. Note that no peak is visible at the chopper frequency (see also text).

Finally, we observe that the August 2017 run marked the first time that a Fabry-Perot based opto-mechanical detector has been used in an actual live data taking run in an astroparticle physics experiment.

The initial sensitivity of the instrument can be improved along the following lines:

1. decreasing the light power circulating in the cavity in order to reduce thermal noise on the membrane
2. cleaning and stabilization of the laser beam modes by pre-injecting the laser beam into a single-mode optical fiber
3. improving the mechanical design of the movement system of one of the cavity mirrors which used in the frequency-locking feedback loop
4. improving the acoustic shielding by employing high-density Mass Loaded Vinyl

We are presently implementing the first two of these improvement steps while the detector is temporarily off-beam.

8 CAST-CAPP

8.1 Achievements in year 2017

Considerable progress has been made since the installation of one cavity in the CAST magnet in autumn 2016, in through the year 2017:

- We demonstrated, for the first time, that a cold dark matter axion search experiment is feasible using microwave cavities in a large dipole magnet:
  - The cavity installed in 2016 remained in stable working condition until the December shutdown, after a number of magnet quenches (Figure 28).
  - The test of a data acquisition system was successfully completed before the same shut-down (Figure 29).

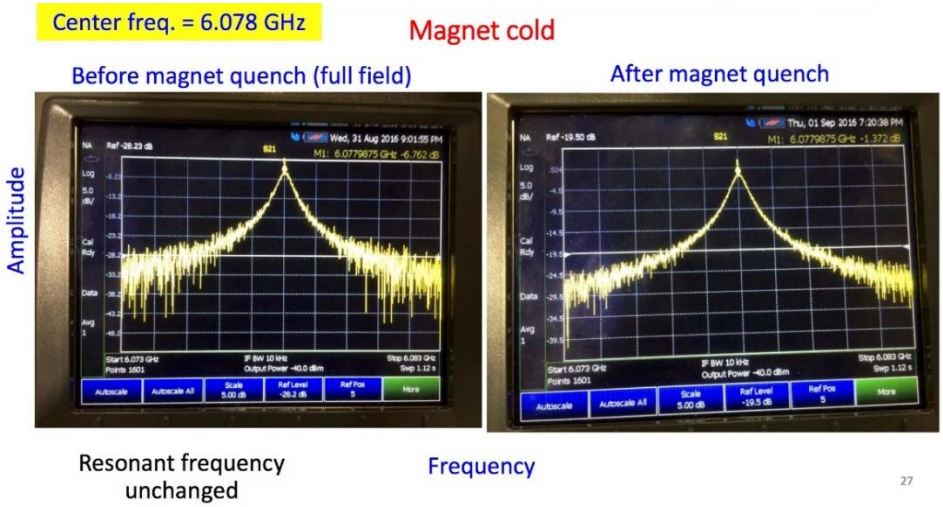

Figure 28: The cavity fundamental resonance frequency is unchanged before and after a quench of the CAST magnet.

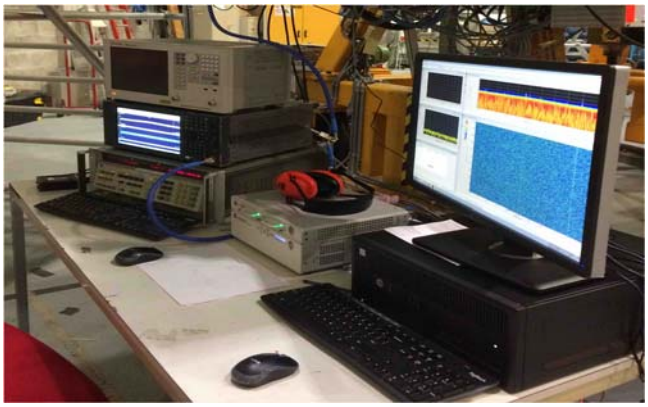

Figure 29: The setup of a test DAQ for the CAST-CAPP Project underneath the CAST magnet in Dec. 2016.

- We have realized, and successfully demonstrated, the all-sapphire tuning mechanism for rectangular cavities. For the demonstration we used a cavity of identical design as the one installed in 2016 (Figure 30 and Figure 31). Extension to the system of four long cavities, to be installed in CAST, is now underway.

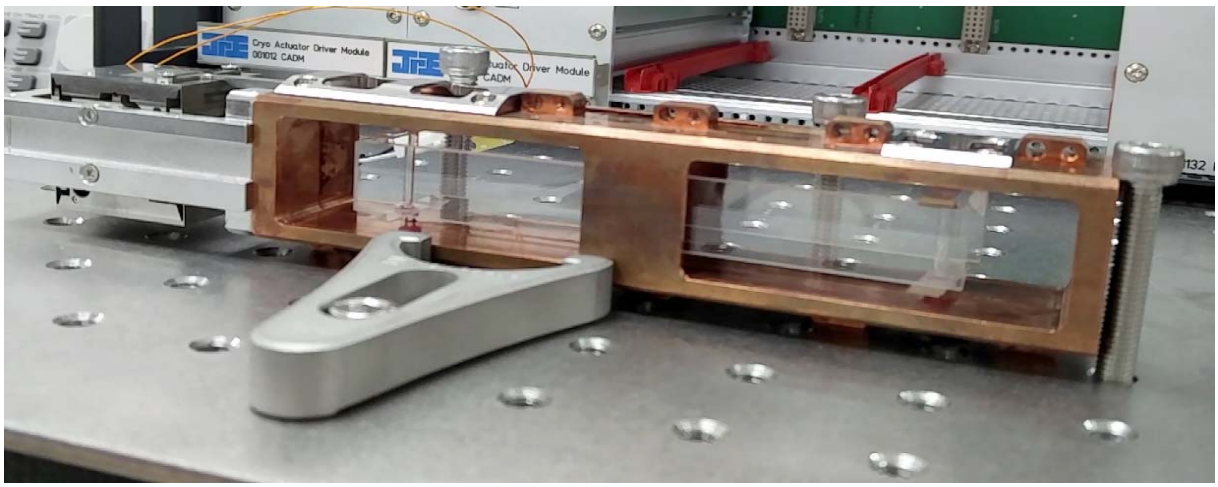

Figure 30: All-sapphire, "locomotive" tuning mechanism in its assembly frame. The piezo actuator, on the left side, couples to the tuner via a locomotive wheel mechanism. One tuner is made of 37 components.

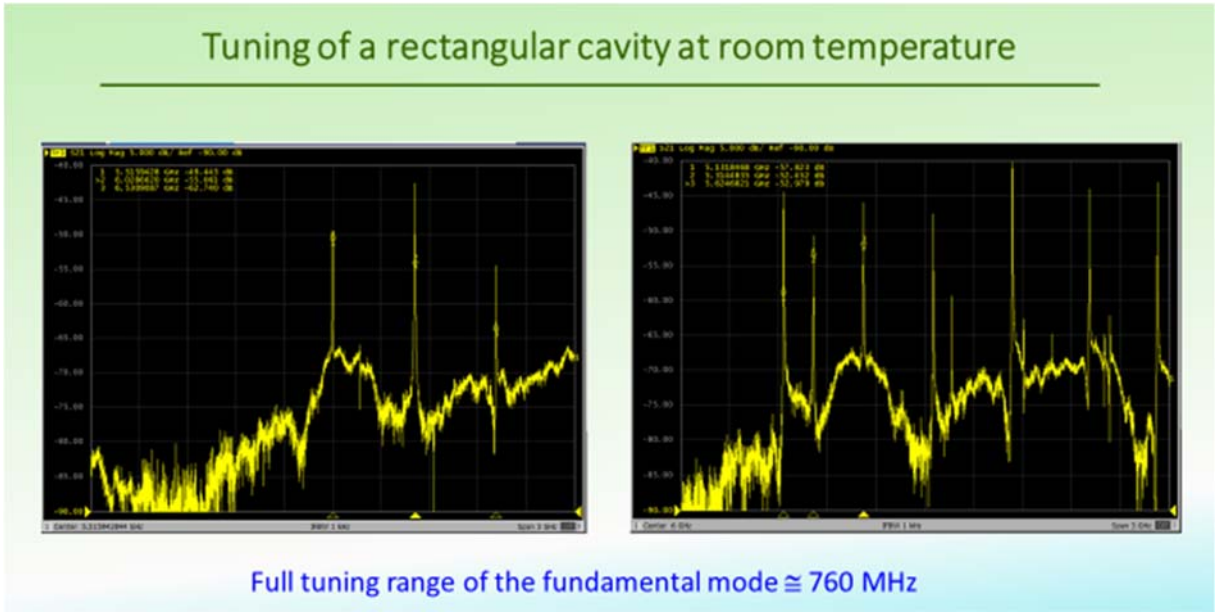

Figure 31: The peaks in this figure represent cavity mode frequencies recorded with a network analyzer from a rectangular cavity of dimensions (23 x 25 x 138) mm³. The "locomotive" sapphire tuning mechanism was loaded in the cavity and driven by a piezo actuator. The first peak from the left, in both images, shows the fundamental mode after moving the tuning plates by half of their maximum range. The full tuning range, as evinced from the figure, is ~ 760 MHz.

- The piezo actuator for the tuning mechanism was successfully tested at low temperatures.
- All components that are necessary for the setup, running, and collection of experimental data are now at hand:
    - All components to assemble, install, and operate a system of four tuneable, phase matched, long cavities inside the CAST magnet.
    - All the necessary DAQ instrumentation.
- A heat load in the magnet bore, originating from the room temperature MFB gate valve window, which prevented the 2016 cavity from reaching thermal equilibrium with the magnet, was identified and corrected for.
- A test comparing three different electroplating procedures, was conducted at low temperature. Based on the test results, the plating job of all new cavities was discussed and scheduled with

the CERN surface treatment lab. This is not expected to impact other activities, since test cavities are available.
- The mechanical system to position, anchor, and retrieve the cavities inside the magnet bore and the thermal link to the bore have been realized, although some refinements may still be necessary.
- The 2D and 3D Hall probes to measure the intensity and orientation of the magnetic field and fringe field, respectively inside and near the bore have been fabricated.

The main difficulties that caused a set back from our original goal for 2017 was a partial redesign and the realization of the tuning mechanism.

8.2 Remaining activities until installation of the detector system inside the CAST magnet

Listed below, are the remaining activities necessary to prepare the installation of the CAPP relic detector system in the CAST magnet:

1. Assembling and testing, at room and low temperatures, of the tuning mechanism for all four long cavities.
2. Electroplating of cavities. It should start in CERN surface treatment lab around mid-October 2017, requiring one month. This is not expected to impact other activities, since test cavities are available.
3. Cavity couplers: build and test
4. DC wiring and RF cabling
5. Test piezo actuators at low temperature and in high B field using a dilution refrigerator.
6. Test of amplifiers in high magnetic field using a dilution refrigerator.
7. Characterization of all RF components
8. Assembling and testing the four cavity system on the bench
9. Preparing and shipping all necessary equipment from Korea to CERN
10. Wiring assembly in cryostat
11. Re-assembling, testing, phase matching at CERN

We plan for the completion of assembling and testing of two initial cavities in 2017 and the remaining two early 2018. Installation and commissioning of 4 phase matched cavities will follow as soon as the magnet is opened in March 2018.

8.3 Sensitivity projections

These updated projections are for an axion mass slightly lower than the one presented in year 2016. This is to reflect the introduction of the dielectric tuning mechanism, which down-tunes the cavity.

As a reference, we consider the HAYSTAC (formerly HDMX-HF), published experiment. This experiment reached 2.3 times the QCD-axion limit, scanning 0.4 micro-eV in roughly 110 days, at expected axion mass m_a=24 μeV.

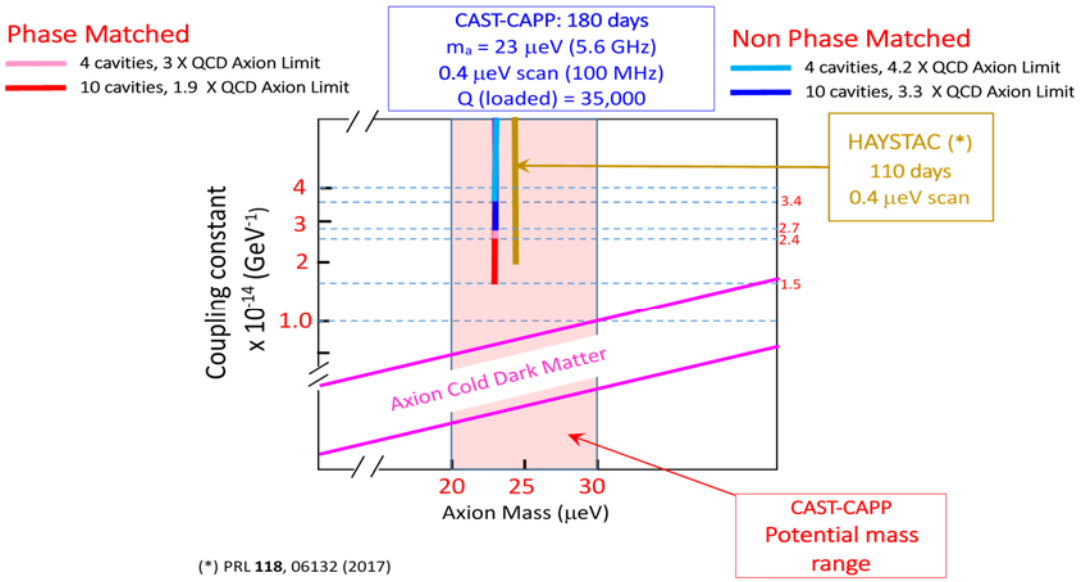

Figure 32: Sensitivity Projections.

CAPP cavities are phase matched as planned:

- With a 4-cavity setup: 2.9 times QCD limit, scanning 0.4 μeV in 180 days, at m_a=23μeV

For comparison:

With phase matching:

- 10 cavity setup: 1.8 times QCD limit, 0.4 micro-eV in 180 days, at m_a=23μeV

Without phase matching:

- 4-cavity setup: 4.1 times QCD limit, scanning 0.4 micro-eV in 180 days, at m_a=23μeV
- 10-cavity setup: 3.2 times QCD limit, 0.4 micro-eV in 180 days, at m_a=23μeV

Axion Streams:

Up to now, in all axion dark matter searches, the axion dark matter density distribution is assumed to be uniform in space and time. However, as more detailed axion distribution models are becoming available, it is becoming clearer, that the possibility of large density fluctuations is likely. In particular, axion streaming / clustering since the origin of the solar system and solar / planetary gravitational focusing of relic axions is of high probability (for a detailed description see ref. [1]). Those fluctuations can boost the axion density up to several orders of magnitude raising the axion detectability provided the axion antenna is sensitive to axion bursts.

On the long term, since the axion mass is unknown, we need to prepare for simultaneous wide axion mass searches around the globe even though with some loss of sensitivity at some station. CAST-CAPP is preparing a port for such a possibility by using wide band electronics to have as wide axion mass range as possible. For this search to be effective a global network needs to be established à la LIGO, starting first collaboration with IBS/CAPP in Korea and later extend it to ADMX, etc. Preliminary discussions have already started agreeing with the principle of the method.

In short, streaming dark matter axions may be the better source for their discovery than the widely assumed isotropic DM.

[1] H. Fischer, Y. Semertzidis, K. Zioutas, *Search for axions in streaming dark matter*, https://ep-news.web.cern.ch/content/search-axions-streaming-dark-matter.
See also http://cerncourier.com/cws/article/cern/69886

8.4 Conclusion

Although we were not able to install the four cavity system by the summer of 2017, we believe that we are well poised to carry on, and successfully conclude, all necessary tasks and activities to commission in March 2018 the CAST/CAPP sub-detector.

9 Detectors: Dark matter axion search with the Relic Axion Detector Exploratory Setup

There is a strong motivation to adapt the conventional axion haloscope (exemplified by the ADMX experiment) to axion mass values above ∼10 μeV. ADMX has demonstrated that this technique is competitive in the 1 to 10 μeV and it has realistic prospects to explore this range down to QCD axion sensitivity in the near future. Pushing these prospects to higher masses is challenging, because it requires to make the cavity resonant to higher frequencies, which means to reduce its volume V, and correspondingly its sensitivity. Several R&D lines are being followed in the community to overcome this issue. One of them is the design of extended periodic structures that could in principle fill large magnetic volumes while coherently resonating at a high frequency, and thus effectively increasing V.

RADES is an exploratory project aiming to test a particular implementation of this concept that is complementary with other similar initiatives in the field, and in particular with the CAST-CAPP project described above. More particularly, the goal is to implement arrays of rectangular cavities coupled with irises, in geometries similar to high-frequency RF filters (although with different design parameters) that could offer good scaling-up prospects and therefore good potential as axion detectors. Although other layouts could be possible, in principle we are interested in one-dimensional cavity arrays, in order to fit the large aspect-ratio of the CAST magnet.

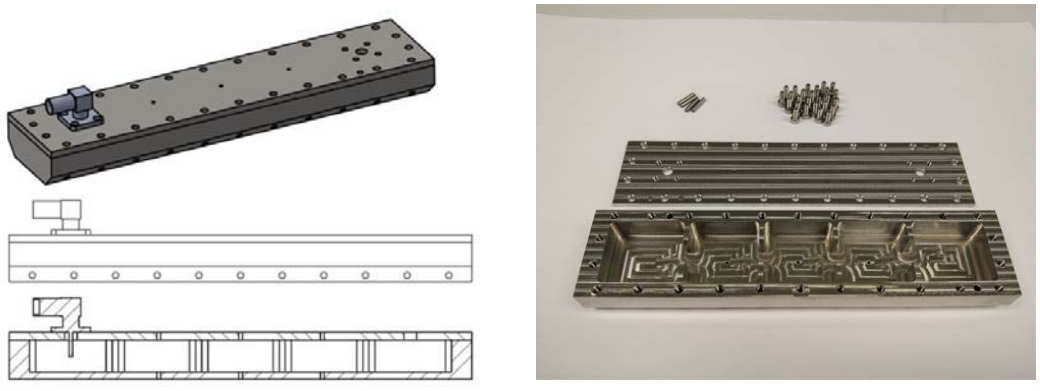

Figure 33: Design (left) and picture (right) of the first RADES cavity recently installed in CAST.

During the previous year, the theoretical framework, as well as generic design prescriptions, were developed. During the last year, a first small-scale prototype has been designed and simulated in detail, built and installed in CAST. The goal of this first step is to face the technical challenges associated with operating this type of setup in the CAST environment and learn from the experience, in order to continue with a more ambitious stage. Consequently, this first prototype is still subcritical regarding it physics potential, although its operation will be representative, in all aspects ranging from hardware installation, cryogenics, calibration, and data acquisition and analysis. This first prototype is composed by 5 sub-cavities, with a total cavity volume of 30 cm^3, and is shown below.

Its fundamental mode (the one coupled to the axion field) resonates at 8.4 GHz and it has no tuning capability. The cavity is built out of stainless-steel, and was coated with a thin layer of copper in the CERN Surface Treatment workshop. A first dry installation in CAST took place beginning of June 2017, to validate the mechanics, length of cables, etc. Final installation inside the CAST magnet happened last July, after which cavity and cryogenic amplifier were enclosed inside the magnet, ready for cool-down. All connections, RF and normal, were transitioned from the cryogenic environment to room temperature and connected to the corresponding feedthroughs. The installation of RADES was completed on the 19th of July. Figure 34 and Figure 35 display a sketch of the setup inside the CAST magnet, and some pictures of the RADES installation in CAST.

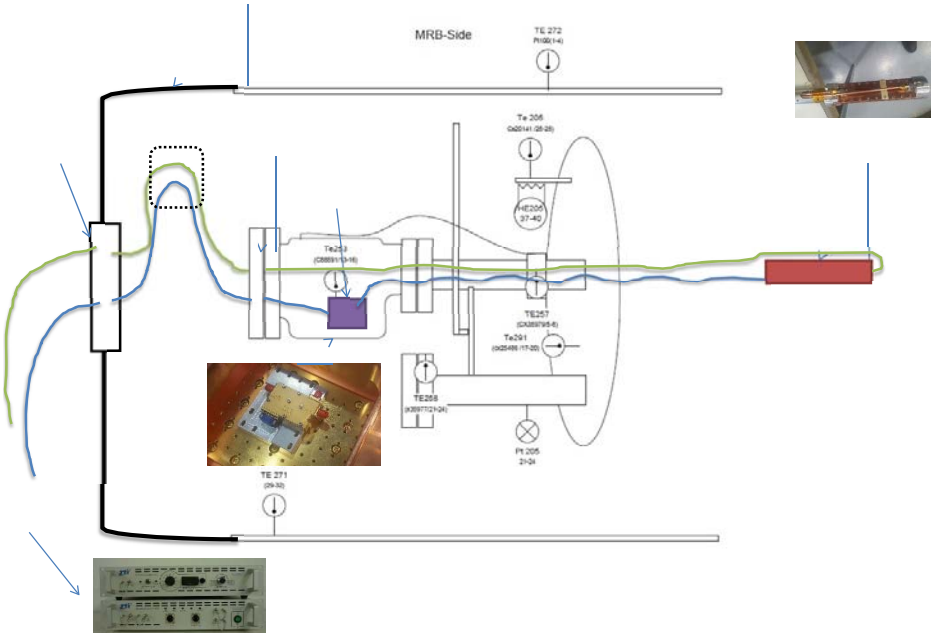

Figure 34: Sketch of the RADES setup inside the CAST magnet.

The remaining system to be placed outside the magnet includes the room temperature data acquisition (DAQ) electronic modules. The system includes a mixing stage, further amplification, sampling, digitization and storage of frequency spectra. The system is in its last stage of assembly. It will be validated during the first week of October and immediately sent to CERN for installation in CAST. The overall system is expected to be ready on time for start of data taking according to the overall timetable of the experiment.

Figure 35: Pictures of the recent installation of the system in CAST.

In overall, the progress of RADES during the last year has been satisfactory according to our planning for 2017, although it still has to culminate with the data taking in CAST. Even if not relevant physics outcome is expected, the data will be analyzed in search for the signal of a dark matter axion, in order to validate the acquisition and analysis protocols. The following Figure 36 shows our expected sensitivity for a campaign of 14 weeks of data taking, assuming the key experimental parameters obtained (Q factor, axion geometric factor, port coupling) are the ones anticipated by simulation of the cavity modes, and a noise figure assumed of 10 K.

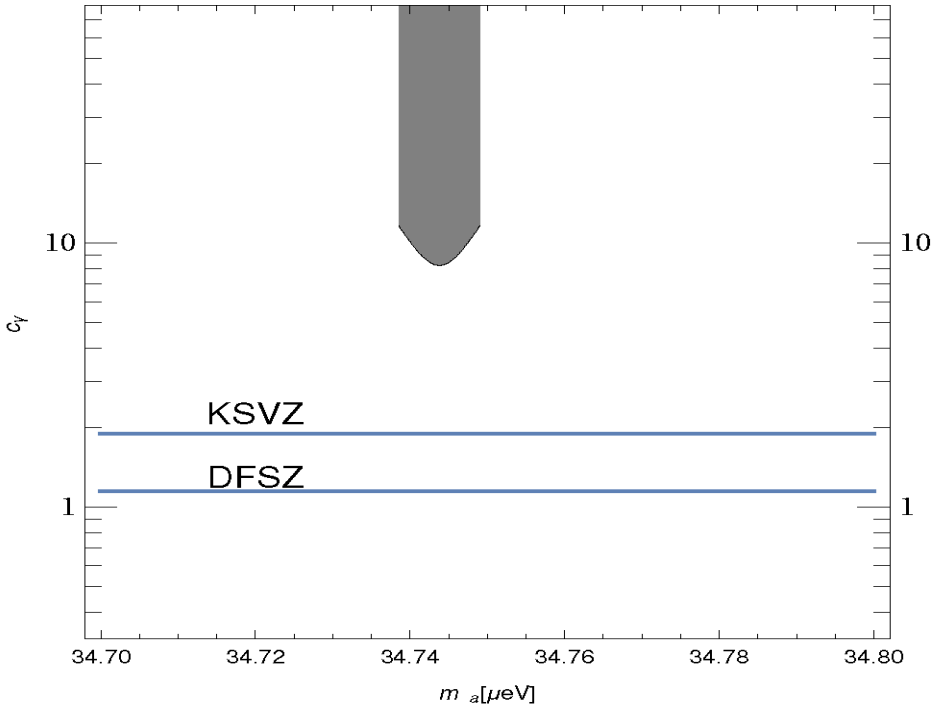

Figure 36: Expected sensitivity with the 2017 setup after 14 weeks of data taking in CAST under the assumptions explained in the text. The y-axis represents the proportionality constant $C\gamma \sim g_{a\gamma}/m_a$ between axion-photon coupling and axion mass.

As is customary, the plot assumes all dark matter density is composed of axions. As can be seen, due to the absence of tuning, the sensitivity is localized on a very thin slice in axion mass. However, despite the modest size of the cavity, the sensitivity is only a factor of a few away from realistic axion models. The technical evaluation of these results will be crucial for the assessment and definition of the next RADES prototype. In addition to all of the above, a scientific article describing the RADES detection concept is under preparation.

The next step of the project for next year is to move to a more ambitious cavity design, applying the experience gathered in the current stage. The design parameters of the new cavity are still to be defined, but generically we aim at implementing one or both of the following:

- A tuning mechanism that allows the system to be sensitive to a certain range of axion masses.
- A larger cavity volume, i.e. larger number of sub-cavities.

Technical details of the tuning mechanism or the extent of the enlargement of the volume are still under discussion. They will depend on the results of the current campaign, the experience gathered and whether new unforeseen technical issues arise. Accordingly it will depend also on the overall CAST plans regarding timetable of next cool-down cycle of the magnet, so that the new step represents a realistic step that can be accomplished with reasonable risks on time for the next campaign in CAST.

10 Preparations for the future

The main activities of CAST (IngGrid, KWISP, CAPP, and RADES) are in full swing. Although these are in our highest priorities, the collaboration has started discussions on future options. In the following we address the year 2018 in line with the rest of this report.

10.1 A new solar axion data taking campaign at the CAST sunrise end with pathfinder technologies for future solar axion experiments

10.1.1 Summary

We propose to resume solar axion searches at the sunrise end of CAST composed by the new LLNL X-ray telescope (XRT), with improved low-background and low-threshold gas detectors (both the microbulk and the InGrid Micromegas detectors). The goal of the proposal is to:

1) improve the result obtained in the 2013-15 phase on $g_{a\gamma}$
2) clarify the statistical/systematic origin of the 2σ-excess observed in the sunrise Micromegas (SRMM) data set;
3) get insight into the limitations of current detection parameters (background and threshold) in both microbulk and InGrid technologies; and
4) provide technical and operational experience for future experimental activities like IAXO or others

10.1.2 Preliminary Considerations

1. The last vacuum solar axion data-taking campaign of 2013-15 has been a success, providing the best limit so far on $g_{a\gamma}$ by CAST. The resulting paper in *Nature Physics* will remain as a legacy publication of the CAST experiment. The improvement with respect to the previous CAST vacuum result has been allowed by the recent achievements on low-background of the Micromegas detectors, plus the construction of a new, axion-optimized, XRT for the SRMM system.
2. In particular, the XRT+SRMM performance has met all expectations. It has proven the combination of both focusing and low-background concepts, previously tested in CAST only separately. This has led to the best signal-to-noise ratio (SNR) of any previous detection system of CAST. The effective background level (number of background counts expected in the energy- and focal-area-region of interest) is of about1count per 6months of operation of the experiment (~0.003 counts/hour).
3. However, the relatively low statistics collected with this system in the 2013-15 campaign (290 tracking hours) makes the result statistics-limited, which partially hinders its impact in the overall limit. In addition, the data revealed 3(4) detected counts in the 95% (99%) signal-enclosing region, while only ~1(~2) was expected. Although this observation can still be a statistical fluctuation of the background (at ~2σ), the possibility of a non-statistical origin of this excess would be very important to dilucidate in view of the low-background limits of this technology. Such a possibility could be tested by additional statistics at CAST.
4. The current understanding of the background limitations of microbulk detectors allow to devise a number of steps to carry out in the quest for even lower background levels. In addition, the past experience with the InGrid detector has demonstrated capability for very low threshold, while the 2017 planned activity will help in applying the low background insight in this technology too. A roadmap of improvements for the InGrid detector is also foreseen. The opportunity of operating these systems at CAST would offer a realistic environment to validate such improvements.
5. In view of the above, it seems desirable to increase data-taking with the SRMM+XRT system. In this section we discuss the motivation, physics and technology-wise, of such a plan, as well as a concrete proposal in this direction.

10.1.3 The solar axion case after the last CAST results

1. The current CAST limit on $g_{a\gamma}$ has reached a value that competes with the best astrophysical bounds (coming from HB stars). This means that CAST is now sensitive to realistic ALP models not excluded by other arguments.
2. Moreover, current CAST sensitivity is bordering the region where models are invoked to solve a number of observational anomalies. The same HB stars limit mentioned above are the upper bound of a result (hint) that mildly favors a hint of non-zero value of $g_{a\gamma}$. Similar hints come also from faster-than-expected cooling rate observed in white dwarfs, RGB and neutron stars.
3. At the low mass part of the parameter space, the current CAST bound borders on the region of values invoked in the issue of the transparency of the Universe to high-energy γ-rays.
4. In view of the above, further improving CAST sensitivity, even if in a modest extent, is a worthwhile effort.

10.1.4 The proposal

1. We propose to re-commission the SRMM+XRT system in CAST (the fact that XRT has been reinstalled already this year together with the InGrid detector will facilitate this action), and plan a new data-taking campaign targeting about ~ 20 months of effective exposure, that could presumably be accommodated in 3 annual campaigns. The total exposure time should be shared between the microbulk and the InGrid detectors. In principle, we aim at at least 13 months of data taking with (at least) similar detection parameters (mainly background level) to ones enjoyed by the microbulk detector in 2015, in order to multiply ×3 the existing SRMM statistics. A small time slot of one or two months could be reserved to test other detectors with similar or better parameters. The concrete periods for InGrid/microbulk would be determined later on by the proponent groups in accordance with the progress and improvement plans on the detectors.
2. The XRT, detectors and shielding are available for reinstallation in CAST and therefore this proposal does not rely on any important investment. The proponent groups need to find resources for maintenance and operation of the systems in CAST during the proposed period, shifts, etc. which seems feasible.
3. A number of technical improvements on the detectors side are under consideration that are being carried out as part of the preparatory phase of future experiments. They could come on time for the campaign in CAST, on a best effort basis. They include:

   <u>For the microbulk detectors:</u>

   a) Change the detector gas to a Xenon mixture, instead of Argon. This may improve the background of the detector (see Figure 37 and its caption). In addition, Xe allows for higher detection efficiency than Ar, and therefore it can be used at lower pressure. A pressure of ~500 mbar of Xe could offer similar efficiency to X-rays that our current 1.4 bar of Ar. This brings two additional practical advantages:1) gas amplification is higher at lower pressures, leading to lower detection energy threshold, and 2) a lower gas pressure puts less mechanical constraint to the window, maybe allowing to go to thinner versions (increasing efficiency to lower energies)
   b) Change to a self-triggered DAQ electronics based on the AGET chip. It will improve the hardware threshold of the detector, currently limited by the high-capacitance (and thus relatively noisy) mesh signal.
   c) Following experience from the InGrid detector, and taking advantage of the small photon entrance by the XRT, go to thinner and smaller windows to decrease detection threshold and increase efficiency at low energies.

   <u>For the InGrid detectors:</u>

   a) Go to larger detector areas (comparable to microbulk detectors), and exploit background reduction obtained by filtering multisite events.

b) Improve low-background capabilities of the detector, both by shielding and radiopurity of components.

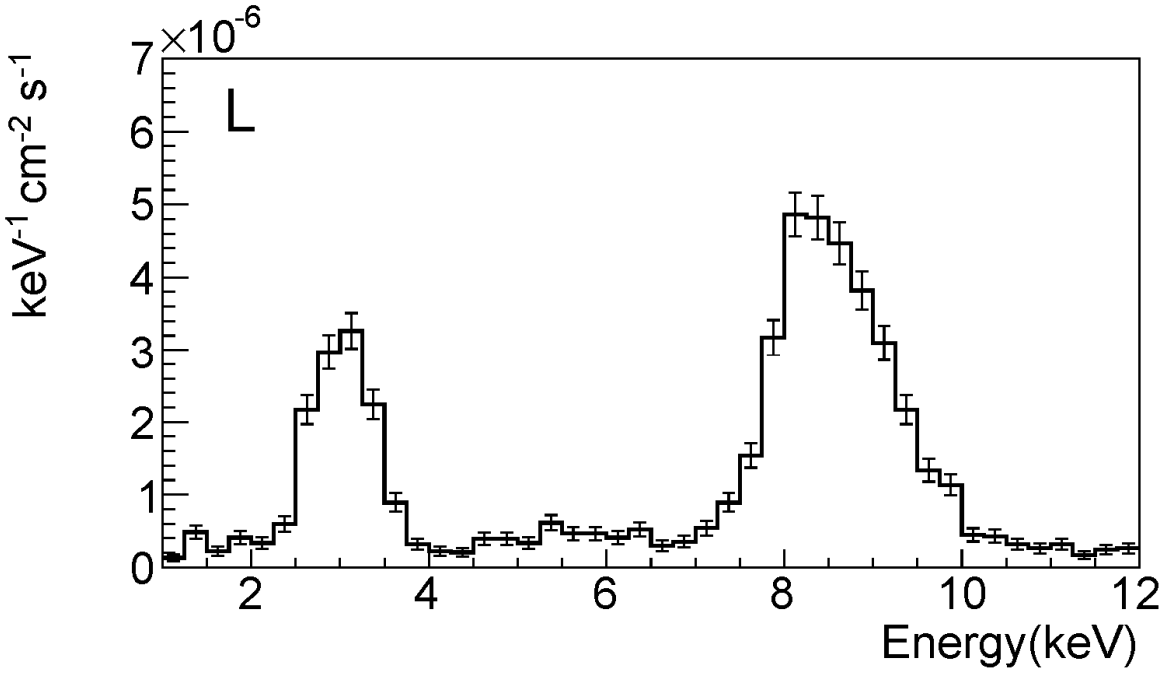

Figure 37: Background spectrum of the SRMM detector during 2015. The peak at ~3keV corresponds to Ar fluorescence and the ~8keV to Cu fluorescence. More than half of the background counts in the 2–7keV region are in the3keV peak. Replacing Ar by Xe in the detector would make this peak disappear and presumably further reduce background. In addition the contribution from the β-decay of the naturally occurring ^{39}Ar isotope, estimated to about 10^{-7} counts/keV/s/cm^2, would be avoided.

10.1.5 Goals

The goals of our proposal can be stated in the following four points:

1. The additional data taken, combined with our previous result, will improve the sensitivity of CAST to $g_{a\gamma}$. Although modest, as argued before, this improvement will further push our current limit into unexplored and interesting values of $g_{a\gamma}$. We consider it worthwhile of the effort and likely to lead to a publishable result. Figure 38 shows the average upper limit expected versus exposure time assuming identical detection parameters (background and efficiencies) as the one of the SRMM+XRT of the 2013-15 campaign.
2. Although the excess observed in the 2013-15 data (see above) is still compatible with a statistical fluctuation of the background, it nevertheless shows a 2-σ tension with background-only expectations. In the event that these counts were of non-statistical origin, its determination would be of utmost importance (in the case of an axion-like signal, for obvious reasons, otherwise because its understanding would be crucial for additional improvements in background). Such a case could be revealed in the data-taking proposed, or alternatively, the fluctuation could be statistically washed out.
3. The recent experience with InGrid detectors demonstrates that very low energy signals (well below keV) are detectable in gas, thanks to the extremely low capacitance of the InGrid pixelated readout (in this respect, current microbulk detectors have been limited by the baseline noise of the high-capacitance mesh electrode used to trigger the detection). In addition, the recent calibration data of the XRT shows good reflectivity figures (and therefore good focusing capability) down to sub-keV energies. This puts the spotlight on the X-ray windows (both the detector and the differential vacuum window), as the main element driving the detection threshold in these systems. This year InGrid will operate without differential window, and with especially developed thin window in the detector. We propose to pursue the quest for lower energy threshold in the new campaign, both with InGrid and microbulks (see technical

improvements above). This could open the window to new steps in sensitivity to other WISP-channels at the low-energy end of the spectrum, like electron-mediated axion production, chameleons, or other –still poorly studied– signals like ALP dark radiation. In addition, the development of low threshold detectors in helioscopes is motivated by the capability of determining the axion mass in some cases of positive detection.

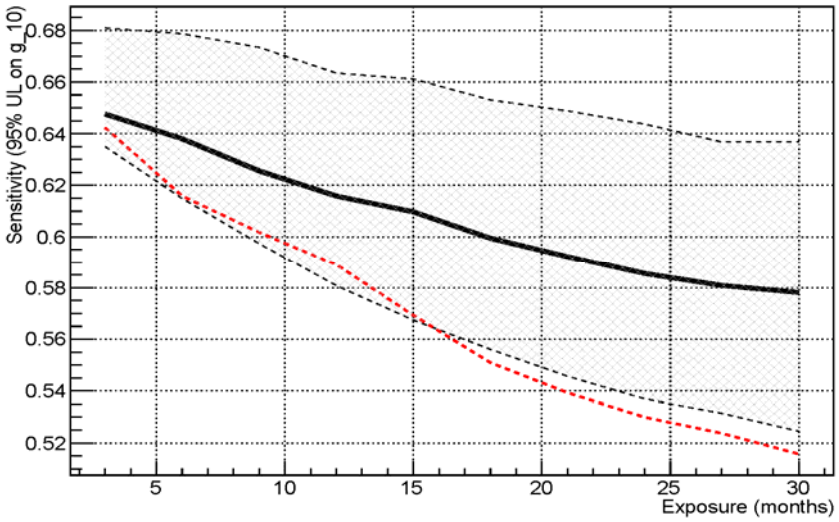

Figure 38: Projected sensitivity of XRT+SRMM system versus the additional exposure considered. The solid black line represents the average upper limit of 1000 statistical outcomes under the only-background hypothesis. The dashed area encompasses the 5% and 95% quartiles of the distribution of upper limits obtained, illustrating the statistical spread expected around the average. The red line represent the upper limit for the case of zero counts detected. The analysis assumes all detection parameters (efficiencies, background level and shape) as the 2015 SRMM system, and takes into account previous CAST results, i.e. it directly shows the improvement expected after a given additional exposure.

4. More generally, the proponent teams are active in developing and implementing new improvements for the detectors, in terms of lower background, threshold and higher efficiency. Some of these have been described above. The operation of both microbulk and InGrid detectors in CAST will be extremely helpful for the consolidation of such improvements, and the exploration for new ones.
5. More in general, the operation of all the systems is of direct interest for a future axion experiment and would allow to produce relevant feedback for the preparatory phase.

10.1.6 Towards Implementation

1. The XRT is already installed at CAST. According to current plan XRT+ InGrid will be operated together in CAST in 2017, anticipating the technical requirements associated with this proposal.
2. The detector systems are also available for this proposal and the responsible teams are currently active in continuously developing improved versions.
3. The proponent groups need to secure the resources needed to maintain the systems in CAST (installation, calibration, etc.) as well as to participate in shifts. This seems feasible if the proposal is positively considered. The proposed activities in Table 1 imply expenses that are covered internally by every group. The proponent groups have the right expertise to cover all needed aspects of the proposal as stated in Table 1.
4. Negotiations with the new groups from IRFU/CEA, DTU, LLNL and Columbia are under way to affiliate with the CAST Collaboration.

Table 1: Contribution of each institute to the programme.

Institution	**Contributions**	**Physicists**
IRFU/CEA	Contribution to the new Micromegas gas system. Installation of the Sunrise Micromegas detector. Responsiblity for detector emergencies. Participation in the data taking. Participation in the data analysis.	I. Giomataris T. Papaevangelou E. Ferrer-Ribas
DTU, LLNL, U Columbia	Contribution to the alignment of the telescope. Ray-tracing codes for the focusing spot position and extension, significance of measured data at a given location in the detectors for current alignment. Participation in the data taking. Participation in the data analysis.	M. J. Pivovaroff J. K. Vogel J. Ruz Armendariz
RBI	Data taking coordination. Participation in the data taking. Participation in the data analysis.	B. Lakic K. Jakovcic
U Bonn	Improved InGrid system. Thin X-ray windows for MM and InGrid. Participation in data taking and analysis.	K. Desch J. Kaminski
U Zaragoza	Operation of the Micromegas detector (calibrations, quick look, data flow). Participation in the data taking. Data analysis.	I. G. Irastorza T. Dafni G. Luzon J. M. Carmona